LIP-STUDENTS-23-20

Obtaining high precision predictions for top-pair production at the LHC in perturbative QCD

André Alves[1,a]

[1] *Faculdade de Ciências da Universidade de Lisboa, Lisboa, Portugal*

Project supervisor: João Pires

November 8, 2023

Abstract. An analysis on the predictions using the Standard Model in perturbative QCD to obtain predictions to the cross section of top-pair production at the LHC. Comparisons between the predictions and the measurements from the CMS and ATLAS detectors will be discussed. The impact of various uncertainties will be evaluated and compared to experimental uncertainties, results from multiple PDF's will be studied and matched with the values of the many runs of the LHC.The results of the experiments are consistent with the SM predictions.

Keywords: LHC, Top quark, Top++

1 Theoretical introduction

1.1 Top quark decay

The top quarks are unstable and can only decay through the weak force, although they also interact with the strong and electromagnetic forces. In the latter cases, the decay is forbidden due to the global symmetry of quark flavour-conservation of the interaction. However, in the weak force decay, with the emission of a W^+ boson, the top quark can decay into one of three possible quarks: down, strange, or bottom.

The probability of each of these decays occurring is proportional to the square of the corresponding CKM matrix element that describes quark mixing in the Standard Model. In other words, the probability of a given quark i decaying into a j is proportional to $|V_{ij}|^2$. The CKM matrix is as follows:

$$\begin{bmatrix} V_{ud} & V_{us} & V_{ub} \\ V_{cd} & V_{cs} & V_{cb} \\ V_{td} & V_{ts} & V_{tb} \end{bmatrix}$$

where the values related to V_{td} and V_{ts} were determined experimentally, being $|V_{td}| = (8.4 \pm 0.6) \times 10^{-3}$ and $|V_{ts}| = (42.9 \pm 2.6) \times 10^{-3}$.Using the unitarity property of the CKM matrix we obtain that $|V_{td}|^2 + |V_{ts}|^2 + |V_{tb}|^2 = 1$ which yields the value $|V_{tb}| = 0.999$.

Thus, the top quark predominantly decays into a bottom quark plus a W^+ boson. The lifetime of the top quark can be calculated using the relationship $\tau = \frac{1}{\Gamma}$, where Γ represents the total decay rate. In the case of a two-body decay, where particle a decays into particles 1 and 2, in the rest frame of particle a, it is given by

$$\Gamma_{fi} = \frac{p^*}{32\pi^2 m_a^2} \int |M_{fi}|^2, d\Omega \tag{1}$$

with the following equation for the momentum

$$p^* = \frac{1}{2m_a} \sqrt{[m_a^2 - (m_1 + m_2)^2][m_a^2 - (m_1 - m_2)^2]} \tag{2}$$

It is then necessary to calculate the matrix element M_{fi}. One significant difference between the weak interaction and strong/electromagnetic interactions is that parity is not conserved, which means that the equation describing the interaction vertex does not have the same form as the other two. From the Dirac equation, we find that the probability density for QCD and QED is of the form $j^\mu = \overline{\psi}\gamma^\mu\phi$, which preserves parity. For the weak interaction, it must be of the form $j^\mu = \overline{\psi}\gamma^\mu\gamma^5\phi$ to be a Lorentz invariant and not preserve parity. Thus, the most general form for the interaction under study is $j^\mu = \overline{u}(p')(g_V\gamma^\mu + g_A\gamma^\mu\gamma^5)u(p)$. Experimental evidence shows maximum parity violation, which implies that $|g_A| = |g_V|$, and it is also observed that weak interaction due to the emission of a W boson is of the (V-A) type, i.e., of the form $\gamma^\mu - \gamma^\mu\gamma^5$, and it is obtained that

$$j^\mu = \frac{g_W}{\sqrt{2}}\overline{u}(p')\frac{1}{2}\gamma^\mu(1-\gamma^5)u(p) \tag{3}$$

The matrix element is then given by:

$$M = \frac{g_W}{\sqrt{2}}\epsilon^*_\mu(p_W)\overline{u}(p_b)\frac{1}{2}\gamma^\mu(1-\gamma^5)u(p_t) \tag{4}$$

In the rest frame of the top quark, you can replace $\frac{1}{2}(1-\gamma^5)$ with the chirality projector P_L and, by its properties, and in the limit where the bottom quark's mass is negligible and its energy is approximately its momentum, the only helicity state in which the bottom quark can be produced is the left-handed one, such that:

$$u_\downarrow(p_b) = \sqrt{p^*}\begin{pmatrix} 0 \\ 1 \\ 0 \\ -1 \end{pmatrix} \tag{5}$$

In this frame and in the limit where the bottom quark's mass is negligible, we have $E_t = m_t$, $E_b = p^*$, and $E^{*2} = (p^*)^2 + m_t^2$ where E^{*2} is the energy of the W boson. Thus, the two possible spin states for the top quark are:

$$u_1(p_t) = \sqrt{2m_t}\begin{pmatrix} 1 \\ 0 \\ 0 \\ 0 \end{pmatrix} \tag{6}$$

[a] e-mail: alvesandre158@gmail.com

$$u_2(p_t) = \sqrt{2m_t}\begin{pmatrix}0\\1\\0\\0\end{pmatrix} \tag{7}$$

There are three possible polarization states for the W boson:

$\epsilon^*_+(p_W) = -\frac{1}{\sqrt{2}}(0,-1,-i,0)$

$\epsilon^*_-(p_W) = \frac{1}{\sqrt{2}}(0,1,i,0)$

$\epsilon^*_L(p_W) = \frac{1}{m_W}(-p^*,0,0,E^*)$

Substituting the spinors 5,6 and 7 into the probability density equation 3, you obtain two possible densities, j_1 and j_2, with their respective indices for the top quark's spinor. Therefore, there are only two combinations of density and W boson polarization states for which the matrix element is nonzero, these being:

$M_1 = \frac{g_W}{\sqrt{2}}\epsilon^*_+(p_W)\cdot j_1 = -g_W\sqrt{2m_t p^*}$

$M_2 = \frac{g_W}{\sqrt{2}}\epsilon^*_L(p_W)\cdot j_2 = -\frac{g_W}{m_W}\sqrt{m_t p^*}(E^*+p^*)$

So the matrix element will be the average of the two, and substituting it into the decay rate equation 1, we obtain:

$$\Gamma(t\to bW^+) = \frac{p^*}{32\pi^2 m_a^2}\int\langle|M|^2\rangle\, d\Omega =$$
$$= \frac{p^*}{32\pi^2 m_a^2}4\pi\times\frac{1}{2}(|M_1^2|+|M_2^2|) =$$
$$= \frac{g_W^2 p^{*2}}{16\pi m_t}\left(2+\frac{m_t^2}{m_W^2}\right)$$

Substituting p^* with its expression given by 2, considering that $m_b << m_W$, and also substituting g_W^2 with $\frac{8m_W^2 G_F}{\sqrt{2}}$, where G_F is the Fermi constant, we arrive at the equation:

$$\Gamma(t\to bW^+) = \frac{G_F m_t^3}{8\sqrt{2}\pi}\left(1-\frac{m_W^2}{m_t^2}\right)^2\left(1+\frac{2m_W^2}{m_t^2}\right)$$

with $m_t = 173GeV$,$m_W = 80.4GeV$ and $G_F = 1.166\times10^{-5}GeV^{-2}$, the total decay rate is $\Gamma = 1.5GeV$ and the top quark lifetime is $\tau = 5\times10^{-25}$ s [1].

1.2 Top quark production at the LHC

There are many ways to produce top quarks at the LHC through high energy proton-proton collisions. In particular, there is a probability that these collisions will create a top-pair, i.e., a top quark and an anti-top quark. The most predominant way for this process to occur is by the strong force and not for example the electromagnetic, this is explained by the higher value of the strong force coupling constant ($\alpha_s \sim 0.118$) when compared to its electromagnetic counterpart ($\alpha \sim \frac{1}{137}$). The strong force coupling constant decreases with the energy of the interaction but its still more than two orders of magnitude bigger than the electromagnetic constant at the levels of center of mass energy of the LHC. Its possible to visualize the production of top-pairs via the strong interactions in the gluon-gluon channel and the quark anti-quark channel with the Feynman diagrams shown in Figure 1 and Figure 2 respectively.

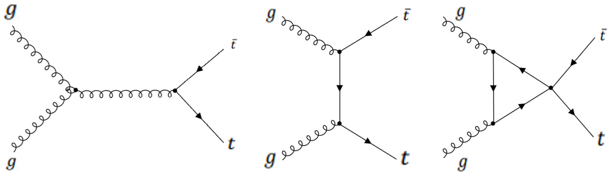

Figure 1. Feynman diagrams for the top quark production via the $gg\to t\bar{t}$ process

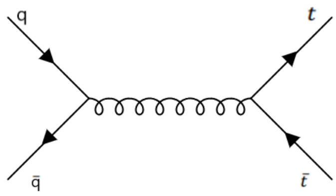

Figure 2. Feynman diagram for the top quark production via the $q\bar{q}\to t\bar{t}$ process

1.3 Renormalization and factorization scale

In order to calculate the cross section for top pair production at the LHC, i.e., to obtain a measure of the quantum mechanical probability for this reaction, we will make use of the program top++ [2], which calculates the diagrams in Figures 1 and 2, and includes higher order QCD corrections to the process up to the second order, i.e., NNLO in the QCD perturbative expansion. For this calculation the program needs to know as an input the value of the coupling strength of the strong force at the Z-boson mass. Subsequently it will use the renormalization group equation to evolve it to the mass of the top quark. Due to this effect and to estimate the theory uncertainty in the calculation from the renormalization scale (μ_R) choice, the program varies μ_R by factors of 2 and $\frac{1}{2}$ around the top quark mass to obtain the spread in the cross section due to this variation, which we will use to represent the μ_R scale uncertainty.

The program also uses PDF's (Parton density functions) that model the distribution of an proton's momentum over all its elementary particles such as quarks and gluons. Each particle has a fraction x_p of its proton's momentum, and with that, the program calculates the cross section of a collision based on the momentum of the two protons (Energy of center of mass), its PDF and a factorization scale (μ_F) that separates Non-Perturbative PDF dynamics from the hard scattering process, which, similarly to the renormalization scale takes as the central value the mass of the top quark and it is subsequently varied by a factor of 2 and $\frac{1}{2}$ around the central value to estimate the theory uncertainty.

Being a proton-proton collider, the LHC mainly produces top quarks by two gluons interacting rather than a quark and an anti-quark, the reason is that at high levels of energy of center of mass ($\sqrt{S}$), the gluons inside the protons carry more of a fraction of proton momentum than the anti-quarks, resulting in a 90% rate of gluon-gluon top quark production and only 10% of quark-anti-quark.

2 Cross section calculation

To calculate the cross section it is also required to specify the desired order of the calculation, using only the leading order (LO) the program only takes first-order Feynman diagrams into account (shown in Figures 1 and 2) which leads to large uncertainties as will be shown in this section. For this reason, to get a better theoretical precision it is necessary to calculate the cross section including higher orders terms. The results for the cross section can be estimated by the following perturbative expansion:

$$\sigma = \sigma_{LO} + \frac{\alpha_S}{2\pi}\sigma_{NLO} + \frac{\alpha_S}{2\pi}^2 \sigma_{NNLO}$$

By plotting the ratio of cross sections from a higher order to a lower one as a function of $\sqrt{S}$ it is possible to check the convergence of the perturbative expansion. This is shown in Figure 3 (using top++[2]) for the NLO result (in red) and the NNLO result (in blue). We observe that the NLO QCD corrections are of the order 40 – 50% while the NNLO correction is of the order of 12%.

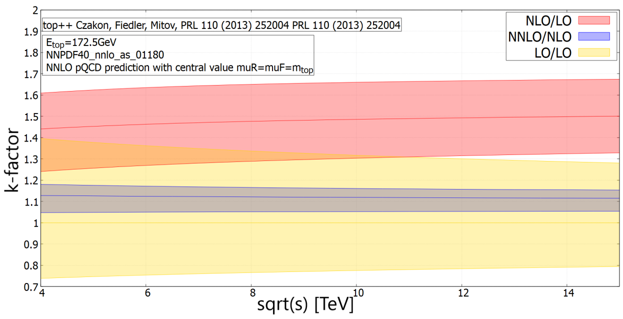

Figure 3. Theory uncertainty on the k-factor in perturbative QCD at LO, NLO and NNLO on the top pair inclusive cross section as a function of the center of mass energy

The plot in Figure 3 also shows an approximately flat dependence of the radiative corrections on the center of mass energy of the proton-proton collision. The bands on the plot represent the uncertainty coming from the renormalization and factorization scale dependence of the predictions, the lower the order, the wider the interval. To visualize this uncertainty better, the plot in Figure 4 shows the variation of the cross section with μ_R on the x- axis and μ_F as the width of the bands.

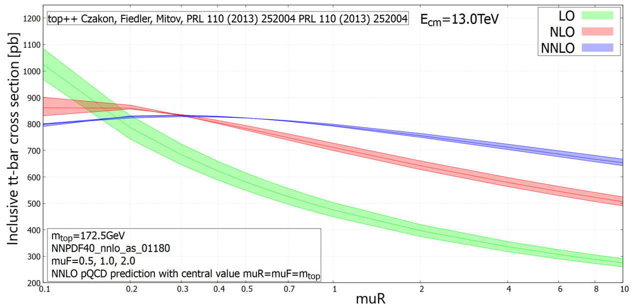

Figure 4. Theory uncertainty on the top pair inclusive cross section from variations of the renormalization and factorization scales

As seen in Figure 4 the μ_F uncertainty bands are indeed thinner as we increase the perturbative order of the prediction. Similarly, the dependence of the cross section on μ_R becomes flatter at higher orders. For phenomenological studies the most relevant range of μ_R is between 0.5 and 2 times the mass of the top quark, and those are the values μ_R will take on the subsequent plots presented in this report. In that range the blue curve (NNLO) is significantly more precise than its green and red counterpart, both in μ_F uncertainty and μ_R uncertainty.

3 Comparison of QCD predictions with ATLAS and CMS data from the LHC

Now with the uncertainties explained its finally possible to show in Figure 5 the comparison between the predictions obtained using the top++ program [2] with the NNPDF40_nnlo_as_01180 PDF set and the measurements performed at the LHC by the ATLAS and CMS experiments.

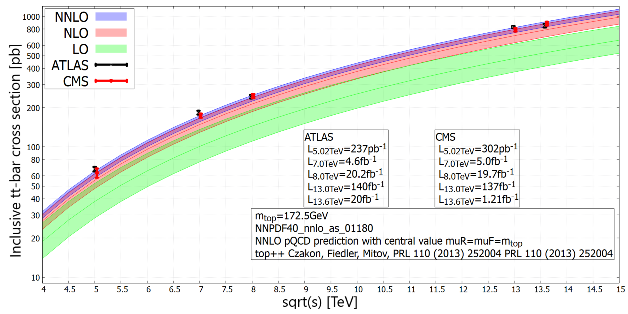

Figure 5. Theory prediction in perturbative QCD at LO, NLO and NNLO for the top-pair inclusive cross section and ATLAS and CMS measurements as a function of the center of mass energy.

We can observe in Figure 3 that with the exception of the data points at $\sqrt{S}$ = $5.02 TeV$ all the measurements have an experimental uncertainty smaller than the scale uncertainty interval computed by the top++ program at NNLO. Moreover, we can observe that the predictions using only LO are systematically below the uncertainty intervals of the measurements. We can observe in the Figure that the NLO and NNLO corrections are positive (as discussed in Figure 3) and bring the theory prediction closer to the experimental data. Overall we observe an excellent description of the top-pair production inclusive cross section as a function of the center of mass energy at NNLO, whose cross section values lie inside the scale uncertainty of the NLO prediction which shows a good convergence of the perturbative expansion.

The plot also presents the values of the integrated luminosity of each measurement. This luminosity factor represents the amount of data recorded by the detector, and the higher the integrated luminosity is, the smaller the statistical uncertainty of the measurement will be. The integrated luminosity values are not all equal due to the different duration times and running conditions that the LHC operated at certain $\sqrt{S}$.

For example the $13.0TeV$ run of the LHC lasted for about 3 years with a higher instantaneous luminosity with respect to the lower energy runs thanks to a smaller interval of the protons bunches from $50ns$ to $25ns$ and smaller beam-size, so even when we compare the same amount of running time, the $13.0TeV$ run still managed to gather more data. This means that it is expected to observe a big difference in the statistical uncertainty with $13.0TeV$ compared to the other center of mass energies. This will be shown in the next plots that show these measurements with their statistical and systematic uncertainties but now compared to the PDF and μ_R and μ_F uncertainties.

To estimate the PDF uncertainty of the theory calculations we will consider changing the PDF set in the predictions and moreover, besides including the member 0 of each PDF set, which corresponds to the best PDF fit, we will also evaluate the cross section using the additional members that represent the PDF fit uncertainty of a given set. Typically a given PDF determination contains approximately 100 members that we evaluate to assess the PDF uncertainty of each PDF set for the top-pair cross section observable and we subsequently compare it to the perturbative μ_R and μ_F uncertainties.

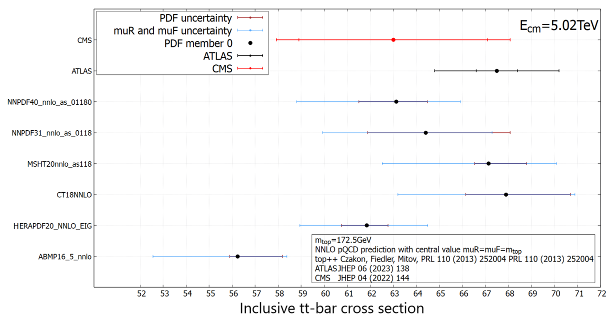

Figure 6. Theory prediction and PDF uncertainty in perturbative QCD at NNLO for the top-pair inclusive cross section and ATLAS[3] and CMS[4] measurements for $\sqrt{S} = 5.02TeV$.

In figure 6 we show all these uncertainties on the NNLO cross sections for top-pair production in proton-proton collisions at $\sqrt{S} = 5.02TeV$ for 6 selected PDF sets. For the experimental measurements it will also be shown the difference between the statistical error (smaller inner band) and the total error (statistical+systematic+luminosity) (full outer band), to see which is dominant in each case.

In figure 6 the statistical error is dominant especially in the CMS measurement.As it was shown in figure 5 the ATLAS and CMS measurements are well described by the NNPDF40_nnlo_as_01180 prediction including the μ_R and μ_F uncertainties. In addition, the measured cross section values are compatible with the predictions from all the other PDF sets that were considered. Quantitatively we observe that for each PDF set the PDF uncertainty is smaller than the μ_R and μ_F uncertainties, usually smaller than a 5% error.

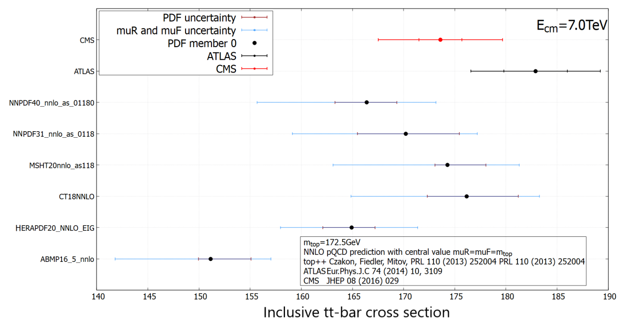

Figure 7. Theory prediction and PDF uncertainty in perturbative QCD at NNLO for the top-pair inclusive cross section and ATLAS[5] and CMS[6] measurements for $\sqrt{S} = 7.0TeV$.

In figure 7, we plot the same variables but now for proton-proton collisions at a center of mass energy of $\sqrt{S} = 7.0TeV$. In this case we can observe that the ATLAS measurement is slightly above the NNPDF40_nnlo_as_01180 prediction as it was seen in figure 5. Similarly to the previous plot, all PDF sets generate consistent predictions with the exception of the ABMP16 PDF set, which has a softer gluon distribution and predicts a cross section value 2.5σ lower than measurement. Moreover, with respect to the previous plot we can observe a significant reduction in the statistical contribution to the total experimental uncertainty, explained by using larger luminosity datasets.

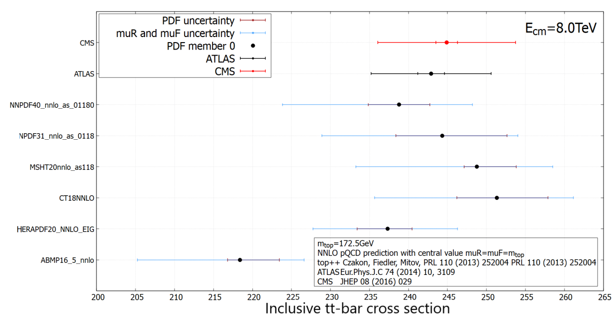

Figure 8. Theory prediction and PDF uncertainty in perturbative QCD at NNLO for the top-pair inclusive cross section and ATLAS[7] and CMS[8] measurements for $\sqrt{S} = 8.0TeV$.

Now plotting for $\sqrt{S} = 8.0TeV$,in figure 8 we see that the measurements from both detectors are the most precise when compared with the theoretical predictions. Being the second runs with the most integrated luminosity, the statistical uncertainty is even smaller than in figures 6 and 7. For the exception of the ABMP16_5_nnlo PDF set, all the PDF's give a good prediction for the cross section.

In figure 9 we performed a data and theory comparison for proton-proton collisions at $\sqrt{S} = 13.0TeV$ where the importance of a bigger luminosity is shown again, namely the statistical error makes up about 6.5% of the total error of the ATLAS measurements and less than 4% of the CMS measurements and the total error is predominantly systematic. For this highly-precise comparison we can see that with the exception of the ABMP16 PDF set, all PDF's give a good prediction for the ATLAS and CMS measurements. In addition, it can been seen on the plot that the dominant uncertainty on the theory side comes from the μ_R and μ_F scale uncertainties which are larger than the experimental uncertainty. This indicates the need for the calculation of higher-order effects beyond NNLO for top pair production at the LHC to reduce the theory uncertainty. As was shown in Figure 3, the NNLO QCD corrections for the inclusive top-pair cross section are of the order of 12% and missing higher order corrections can contribute to further stabilise the perturbative expansion. To this end, it would be desirable to perform a study of the quantitative impact of the available soft-gluon resummation effects to the total top-pair cross section as well as obtaining a full computation at N3LO in QCD for this process, in view of the upcoming High-Luminosity LHC Phase.

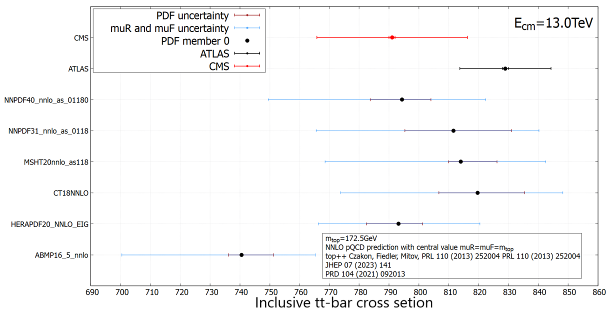

Figure 9. Theory prediction and PDF uncertainty in perturbative QCD at NNLO for the top-pair inclusive cross section and ATLAS[9] and CMS measurements[10] for $\sqrt{S} = 13.0TeV$.

Finally we plot in Figure 10, the latest measurements obtained in 2023 with the first datasets of proton-proton collisions recorded at the highest center of mass energy of $\sqrt{S} = 13.6TeV$. We observe that the increase in center of mass energy from $\sqrt{S} = 13.0TeV$ to $\sqrt{S} = 13.6TeV$ represents an increase in the top-pair cross section of about 10% which originates from the steep rise in the gluon PDF at the lower-x values being probed here. Nonetheless we observe (with the exception of the ABMP16 PDF set) a good consistency between the predictions obtained with the different PDF sets, which are compatible with these new measurements. In addition, we observe a big discrepancy between the portion of statistical error of the ATLAS and CMS measurements as in the ATLAS measurement the statistical error is only a small portion of the total error but in the CMS is the predominant part. This is only due to the ATLAS analysis making use of an integrated luminosity of 29fb^{-1} while the published CMS measurement used an integrated luminosity of 1.21fb^{-1}.

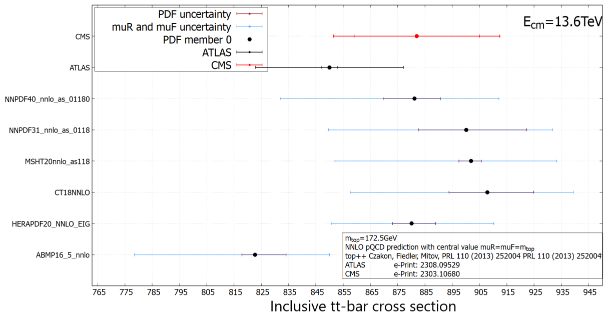

Figure 10. Theory prediction and PDF uncertainty in perturbative QCD at NNLO for the top-pair inclusive cross section and ATLAS[11] and CMS measurements[12] for $\sqrt{S} = 13.6TeV$.

4 Conclusion

To be able to understand the results given by the top++ [2] program, we started by describing the process of top-pair production at the LHC. In particular, the perturbative approach employed in terms of Feynman diagrams was reviewed and it was examined how the renormalization and factorization scale dependence together with the order of the calculation explains the theory uncertainty produced by the top++ [2] program. The importance of calculating the cross section at higher orders in QCD was shown in figure 3 where the higher order effects to the total top-pair production cross section amount to 45% at NLO and 12% at NNLO, which are significantly larger than the experimental uncertainty achieved in the current measurements at the LHC.

In figure 4 we observed that the dependence of the theoretical cross section on both the renormalization and factorization scale is significantly reduced at higher orders which contributes to a reduction in the perturbative uncertainty of this observable.

In the first comparison between the QCD predictions and the data from the LHC shown in figure 5, the calculations using the NNLO result are in good agreement with the experimental data that also lies inside the scale uncertainty of the predictions, showing that in perturbative QCD, the SM precisely predicts the center of mass energy dependence of the top-pair cross section at the LHC. In the same plot we observed that the lower order predictions in the expansion systematically undershoot the measurements in every $\sqrt{S}$ calculated.

Subsequently, we studied the PDF uncertainty for various PDF sets and $\sqrt{S}$ values. The PDF used in the first plots (Figures 3, 4 and 5) was the NNPDF40_nnlo_as_01180. A more detailed analysis was performed including an additional five PDFs sets which made use of all their individual members to evaluate the PDF uncertainty of the predicted cross section at NNLO. Although the ABMP16_5_nnlo PDF set predicts a lower cross section for every $\sqrt{S}$, the remaining predictions are well compatible with each other and contain the experimental data inside the PDF+scale uncertainty band. In all these plots the perturbative scale uncertainty was also shown to be always bigger than the PDF uncertainty, the latter regularly having error smaller than 5%.

In conclusion we observed that, for all the plots describing the top quark pair production cross section, the SM predictions in perturbative QCD made by using the top++ [2] program were consistent with the data obtained from the LHC. Because the current and future high-luminosity measurements of this process aim at significantly smaller experimental uncertainties than the current theoretical input, the next step would be to use an higher order of calculation (N3LO) to predict the LHC and HL-LHC top-pair data with greater precision.

References

[1] M. Thomson, *Modern Particle Physics* (2013)
[2] Top++ Czakon, Fiedler, Mitov, PRL 110 (2013) 252004 PRL 110 (2013) 252004
[3] ATLAS JHEP 06 (2023) 138
[4] CMS JHEP 04 (2022) 144
[5] ATLAS Eur.Phys.J.C 74 (2014) 10, 3109
[6] CMS JHEP 08 (2016) 029
[7] ATLAS Eur.Phys.J.C 74 (2014) 10, 3109
[8] CMS JHEP 08 (2016) 029
[9] ATLAS JHEP 07 (2023) 141
[10] CMS PRD 104 (2021) 092013
[11] ATLAS e-Print: 2308.09529
[12] CMS e-Print: 2303.10680